Processing and Application of Ceramics 9 [3] (2015) 131–138
DOI: 10.2298/PAC1503131A

Synthesis, extrusion processing and ionic conductivity measurements of sodium β-alumina tubes

Karanja Avinash[1], Madireddy Buchi Suresh[2], Asit Kumar Khanra[1], Roy Johnson[2,*]

[1]*Department of Metallurgical and Materials Engineering, National Institute of Technology, Warangal, India*
[2]*International Advanced Research Centre for Powder Metallurgy and New Materials, Hyderabad, India*

Received 4 August 2015; Received in revised form 3 September 2015; Accepted 22 September 2015

Abstract

Pure and Li-doped sodium β-alumina ($NaMg_{0.67}Al_{10.33}O_{17}$) ceramics were prepared from the stoichiometric mixture of raw powders. Pellets and tubes were formed from the precursor (NBA-1S) and preformed sodium β-alumina powder through compaction and extrusion processing, respectively. The obtained specimens were finally sintered to dense ceramics. The ceramics were comparatively evaluated for their density, microstructure, phase formation and electrical properties. Both tubes and pellets processed with the preformed sodium β-alumina powder (NBA-2S) showed enhanced densification along with relatively better phase purity and crystallinity. The ceramics prepared from the preformed powder exhibited higher density of 94–95% TD (theoretical densities) in comparison to the ceramics processed from the raw mixture (NBA-1S) with a density of 85–87% TD, which are complemented well through fractographs and microstructures. The ceramics processed using the preformed sodium β-alumina (NBA-2S) also exhibited high room temperature AC conductivity of 1.77×10^{-4} S/cm (1 MHz) with an increasing trend with temperature. The higher ionic conductivity at all temperatures in NBA-2S than in NBA-1S ceramics can be attributed to the relatively high phase purity, crystallinity and higher density values of NBA-2S ceramics.

Keywords: *extrusion, calcination, microstructure, impedance study*

I. Introduction

Energy storage in modern times focuses on efficiency and innovative technologies. Among such technologies sodium-sulfur (Na-S) batteries which can store energy have been identified as a high efficiency and large duration device [1]. Na-S batteries consist of sulfur as positive and sodium as negative electrode. Beta alumina solid electrolyte (BASE) based batteries were first developed by Ford Motor Company in an attempt to develop their electric vehicles [2–4]. Though encouraging results were reported by several workers during the past, there are issues that hinder its wide technological applications. However, in the context of the current importance in renewable energy sources, interest has been generated in the area of Na-S batteries where sodium β-alumina (NBA) is a key component that determines the performance to larger extent [5,6]. It separates anode and cathode and act as fast ion conducting solid electrolyte. Hence, there is not only scientific but also technical reason to investigate the processing and sintering of sodium β-alumina.

The chemical formula $(Na_2O)_{1+x} \cdot 11\,Al_2O_3$, where x = 0 for stoichiometric sodium β-alumina and could be as high as 0.57 due to excessive sodium resulting in higher conductivity values. Beta alumina is generally characterized by closely packed spinel layers with oxygen ions and aluminum ions in both octahedral and tetrahedral interstices and loosely packed planes which allow sodium ion mobility under electric field [7–9]. However, crystal structure (hexagonal for β-alumina and rhombohedral for β''-alumina) differs according to the chemical stoichiometry and stacking sequence of oxygen ions across the conduction plane. Sodium ion conductivity of β''-alumina with rhombohedral crystal structure is higher in comparison to β-alumina [10,11].

Solid state processing of sodium β-alumina has been generally processed through compaction followed by high temperature sintering. The process is cumbersome especially due to the sodium losses at higher temper-

*Corresponding author: tel: +91 40 24443169,
fax: +91 40 24442699, e-mail: *royjohnson@arci.res.in*

atures. Though, high sintering temperatures are necessary in solid state reaction and allow larger grain size, proper procedure to synthesize the NBA compounds by optimizing the thermal treatments will help in the tube processing and densification of the final product. Solid electrolyte applications generally employ the tubular configurations and hence extrusion forming has been identified as a useful method [12].

Ford Motor company patented extrusion followed by sintering of high density β''-alumina tubes mainly because of the advantages over casting of precursor slurry [2,13]. Cold extrusion with binders such as polyvinylpyrrolidone / ethylene glycol, polyvinyl alcohol, as well as hot extrusion with binders such as beeswax and vaseline etc., were explored for processing of β''-alumina by earlier studies. Generally in ceramic extrusions the powder is mixed with 2–3 wt.% binder, regarding to the total mixture, in a ball mill using alumina balls as the mixing media. The mixture is kneaded into extrudable dough using poly-ethylene glycol as plasticizer in a high shear vacuum sigma kneader to ensure the distribution of binder and hence high homogeneity of the dough. The dough which exhibits a shear thinning rheology and confirms the extrudablity is further extrusion shaped into components with dies of required geometry employing either a ram type or screw type extruder [14,15].

In the present study, an attempt has been made to synthesize phase pure NBA through solid state reaction and to investigate the differences between performances of extruded and sintered tubes obtained from the preformed NBA powder and the stoichiometric mixture of raw powder. In addition, influence of lithium addition on the formation of NBA phase has also been analysed.

II. Experimental procedures

2.1. Sample preparation

The pure and Li-doped sodium β-alumina ($NaMg_{0.67}Al_{10.33}O_{17}$) ceramics were prepared from precursor powders: alumina (Baikowski, France), sodium oxalate (Qualigens, India), magnesium hydroxide (Qualigens, India) and lithium carbonate (Loba Chemie, India). The precursor mixture, obtained from stoichiometric amount of the starting powders (Table 1), was milled in the planetary mill using alumina balls with the charge to ball ratio of 1:1 at 200 revolutions per minute for a duration of 2 h. The obtained precursor mixture was divided into two parts and used for preparation of two different samples, NBA-1S and NBA-2S. The first part was directly used for the formation of green bodies (denoted as NBA-1S), where the second one was formed into wet nodules of 3–4 mm diameter and placed in an alumina crucible embedded in calcined sodium beta alumina powder for preventing Na evaporation and closed with the lid. The samples were calcined between 1400–1500 °C to obtain the preformed powder (denoted as NBA-2S). The precursor powders were also doped with lithium by addition of lithium carbonate and the obtained samples are designated as NBA-1S-Li and NBA-2S-Li.

The prepared powder samples were blended with 3 wt.% of methylcellulose as a binder and subsequently kneaded in a vacuum sigma kneader for about 20 minutes. While kneading polyethylene glycol (1 wt.%) was added as a plasticizer together with water (30 wt.%). Both dough materials were characterized for their rheological properties using an indigenously designed and fabricated capillary extrusion rheometer and the procedure followed is described elsewhere [15]. Extrusion pressure, P, required for maintaining a stable flow through the capillary die were calculated from the steady state load values corresponding to the plateau region of the load displacement curve, as load per unit cross sectional area of the barrel, $(4F/\pi \cdot D^2)$, where F is the load and D is the diameter of the barrel. Similarly, the extrusion velocities, V, corresponding to these pressures were calculated from the ram rates scaled for the relative change in the cross sectional area from the barrel to the capillary, using the following equation $V = v \cdot (D^2/d^2)$, where v is the ram rate and d is the diameter of the capillary die. Shear stress and shear rates were estimated and viscosity values were calculated. The dough was extruded into tubes using the extrusion die mounted on universal testing machine.

The tubes were extruded at different extrusion rates with ram rates of 25–75 mm/min. The samples were dried at 110 °C for 2 h, embedded in powder bed and sintered under identical conditions, i.e. 1700 °C for a period of 1 h and at a heating rate of 3 °C/min. For the sake of comparison, the samples were also prepared by compaction from the same formulations and subjected to sintering under identical conditions by placing the samples in a crucible with a closed lid to avoid the sodium evaporation.

Table 1. Sample notation and composition of precursor powders

Sample notation	Composition [wt.%]				
	alumina	sodium oxalate	magnesium hydroxide	lithium carbonate	preformed NBA powder[a]
NBA-S1	78	18	4	0	
NBA-S1 -Li	78	18	4	1	
NBA-S2					100

[a] obtained by calcination of the raw powder mixture NBA-S1

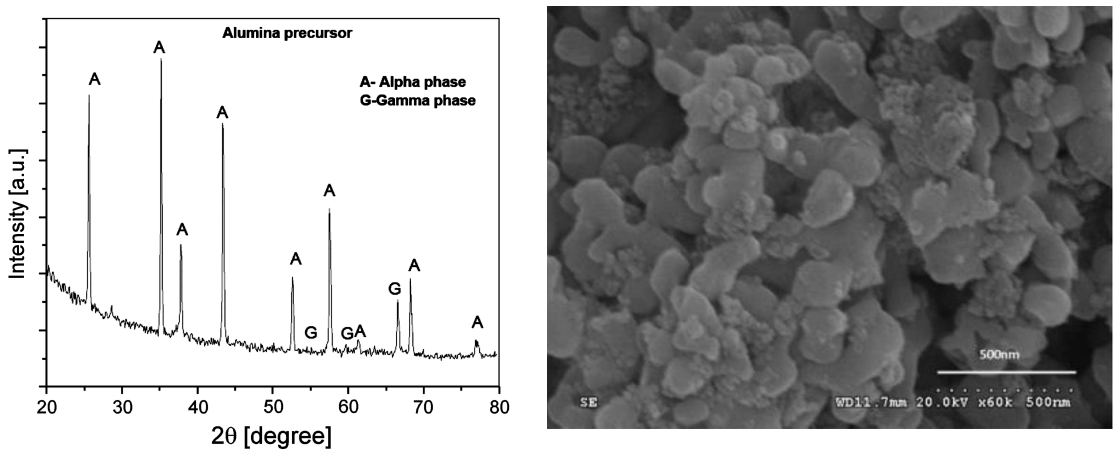

(a) (b)

Figure 1. XRD pattern (a) and SEM micrograph (b) of alumina powder

2.2. Sample characterization

The precursor powders and preformed NBA powder were analysed by X-ray diffraction, XRD (Bruker AXS GmbH, Karlsruhe, Germany) and scanning electron microscopy, SEM (Hitachi, Tokyo, Japan). The sintered tubes and pellet samples were characterized by density measurement using Archimedes principle, microstructural analysis using SEM and AC impedance measurement using Solartron SI1260 Impedance Analyzer. Prior to the electrical measurements from 30 to 500 °C, the surfaces of the sintered discs were polished and coated with silver paste and then annealed at 500 °C for 30 min to remove residual organics. The electrical conductivity was measured by measuring the impedance/admittance of the sample in the frequency range of 1–10^7 Hz at 100 mV AC signal. Platinum mesh and platinum wires were used as current collectors and leads, respectively. The ionic conductivity (σ) was calculated from the impedance data and the activation energy (E_a) of the conductivity was determined by the Arrhenius law: $\sigma \cdot T = \sigma_o \cdot \exp(-E_a/kT)$, where σ_o is the pre-exponential factor and k, the Boltzmann constant.

III. Results

X-ray diffraction pattern and SEM micrograph of the major raw material (alumina) are shown in Fig. 1. The precursor alumina powder exhibited a mixed of alpha and gamma phases. Gamma phase with its inherent defect structure and relatively high surface area in comparison to alpha phase is expected to enhance the reaction rate leading to the formation of NBA phase [16–18]. SEM image of the powder has shown an irregular morphology. Purity of sodium oxalate contributing was found to be 99.5% which ensures decomposition resulting in no residual impurities.

XRD patterns of NBA and Li-doped NBA powders calcined at 1500 °C are shown in Fig. 2. It is evident that the un-doped powder calcined at 1500 °C exhibited the pure NBA phase indicating the retention of sto-

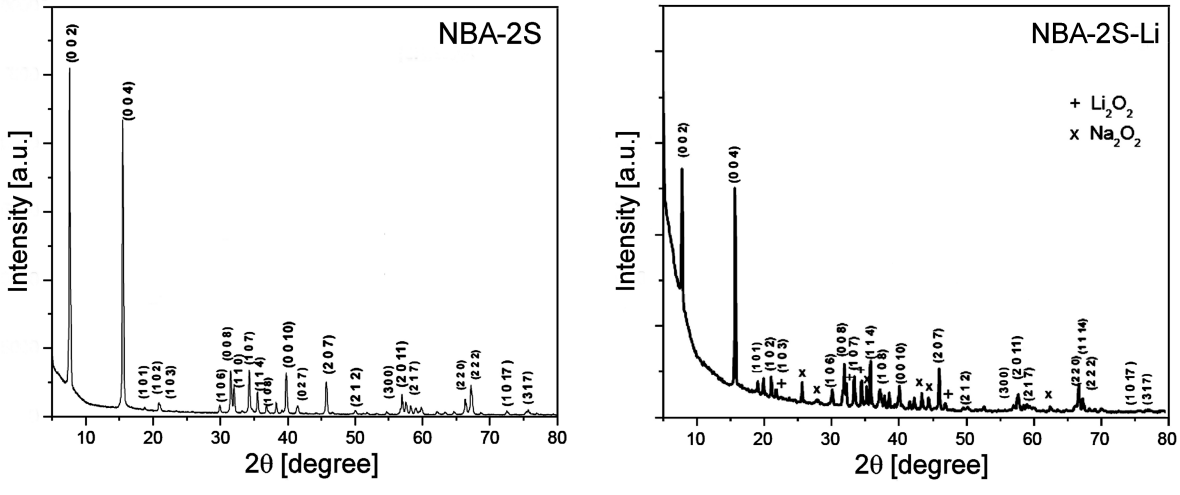

(a) (b)

Figure 2. XRD patterns of: a) NBA and b) Li-substituted NBA powders calcined at 1500 °C

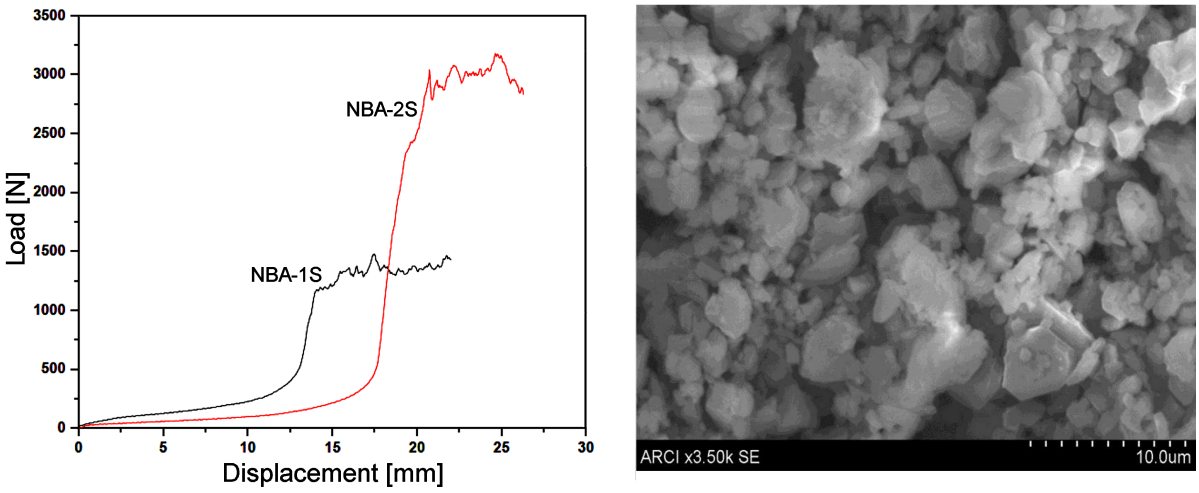

(a) (b)

Figure 3. Load versus displacement curves (a) and SEM morphology (b) of NBA-S2 powder calcined at 1500 °C

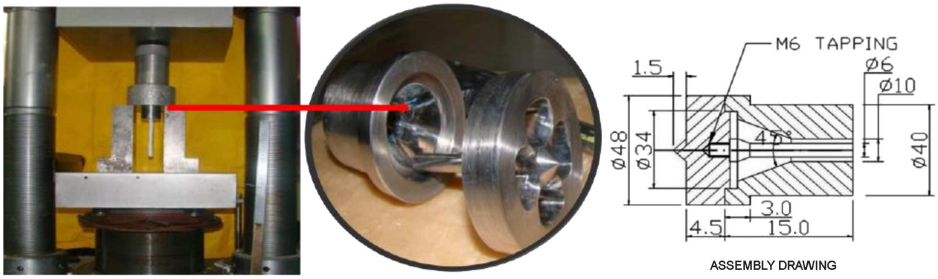

Figure 4. Extrusion process and tool assembly/design

ichiometry with minimum losses in sodium which may be attributed to the powder bed encapsulation. This is further evident from the EDS analysis of the samples exhibiting the presence of sodium in the stoichiometry. Though, Li substitution has resulted in formation of undesirable phases, thus, the peaks corresponding to residual oxides such as Li_2O_2, Na_2O_2 and Al_2O_3 were also observed. This may be due to the presence of excess Li and Na salts in the initial formulation or incomplete formation of NBA [16–18]. According to this, further studies were limited only to the un-doped NBA-1S and NBA-2S samples with magnesium hydroxide as the additive in view of the stabilization of NBA phase. Typical load versus displacement curves recorded for the raw mixture (NBA-1S) and NBA calcined at 1500 °C (NBA-2S) are shown in Fig. 3a. Calcination enhances the load required for extrusion significantly; however, the extrusion process is almost consistent in both the cases showing an identical behaviour after the ejection from extruder. This can be attributed to the surface morphology (Fig. 3b) of the calcined powder with occasional agglomerates, which enhances the inter-particle friction.

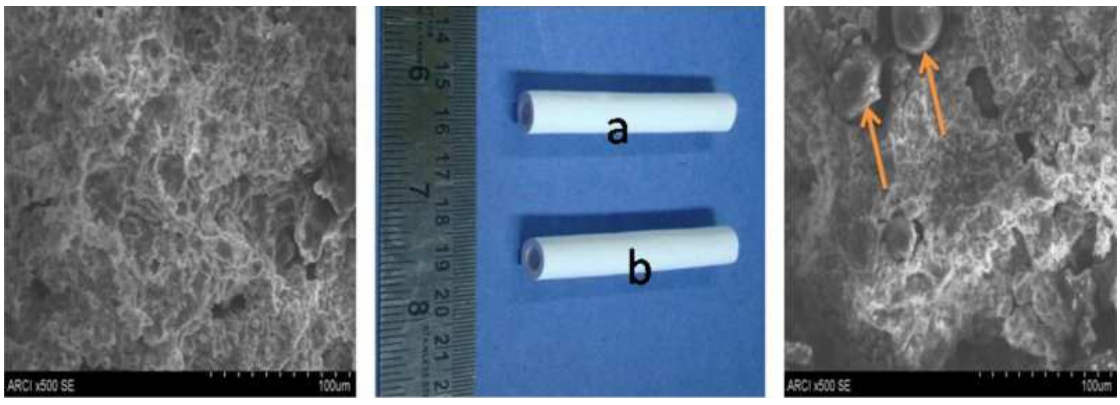

(a) (b)

Figure 5. Extruded NBA tubes and corresponding SEM micrographs: a) NBA-1S and b) NBA-2S ceramics (arrows indicating the unbroken granules)

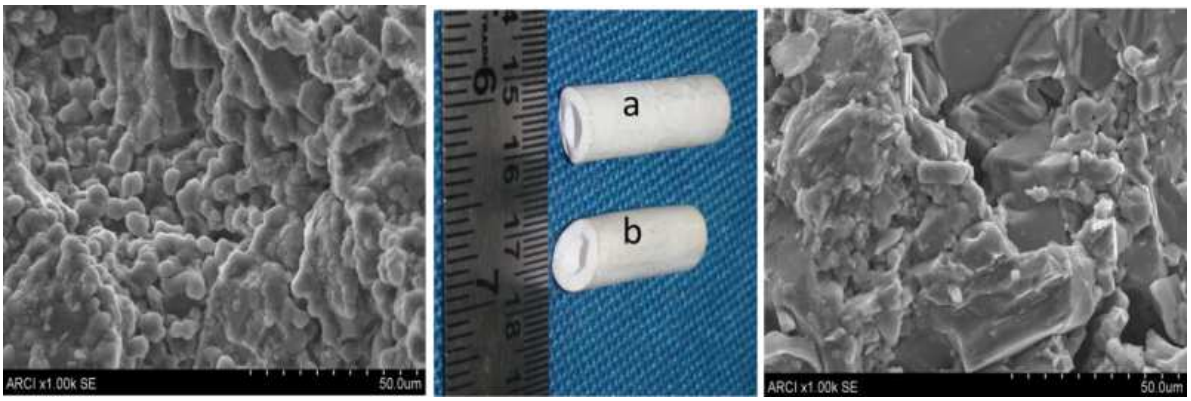

(a) (b)

Figure 6. Sintered NBA tubes and corresponding SEM micrographs: a) NBA-1S and b) NBA-2S ceramics

Table 2. Densities of sintered sodium beta alumina tubes and pellets

Sample	Density of pellets		Density of tubes	
	[g/cm^3]	[%TD]	[g/cm^3]	[%TD]
NBA-1S	2.73	85	2.79	87
NBA-2S	3.02	94	3.05	95

Typical extrusion process and tool assembly are shown in Fig. 4. A cone angle of 45° and a die land of 15 mm (that are evident from the assembly drawing) are employed for extrusion processing of the dough. Extruded tubes and the SEM images of the fractured surface of the samples are shown in Fig. 5. The extruded tubes found to be devoid of any common visible extrusion defects. SEM micrograph of NBA-1S tubes, shown in Fig. 5a, exhibit a well packed structure resulting in the merging of particles in the green samples. However, the SEM fractograph of NBA-2S samples (Fig. 5b) shows unbroken agglomerates even after kneading and extrusion. The sintered tubes along with the microstructure of the fractured surfaces are shown in Fig. 6. It is evident from Table 2, that the pellet and tube, processed with NBA-2S route, achieved a density of 94–95% TD (theoretical density). However, the pellets and tubes, processed with NBA-1S route, exhibited relatively low densities of 85–87% TD. Initial formation of NBA at high temperatures of 1500 °C in the case of NBA-2S sample is expected to reduce the sinterability of powders in comparison to the raw mixture (NBA-1S sample). The lower density of NBA-1S ceramics can be attributed to decomposition of oxalate and generation of significant amount of CO_2 which makes the pellet highly porous and decrease the densification [18]. On the other hand, the density of NBA-2S ceramics was limited to 95% TD probably due to unbroken agglomerates left even after kneading and extrusion, as it can be seen Fig. 5b.

The sintered NBA-2S tubes contain lower portion of porosity (Fig. 6b) than NBA-1S sample (Fig. 6a) and have faceted grains. The fractographs are in line with

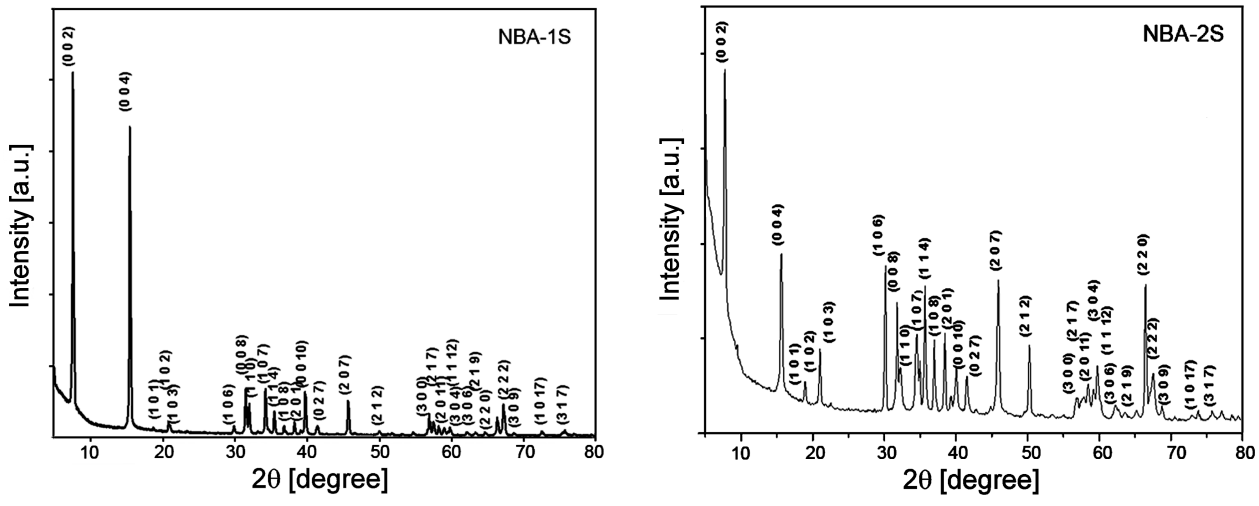

(a) (b)

Figure 7. XRD patterns of: a) NBA-1S and b) NBA-2S ceramics

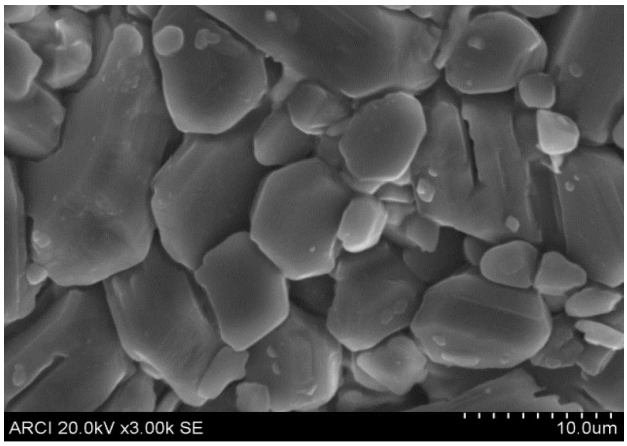

Figure 8. Microstructure of NBA-2S ceramics (polished surface)

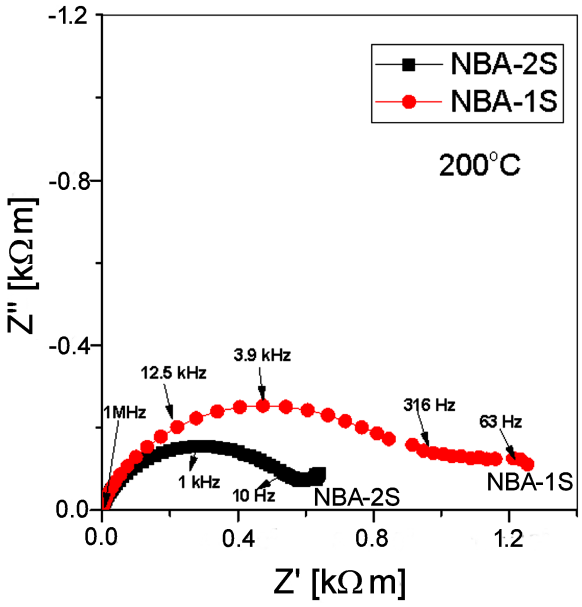

Figure 9. Cole-Cole plots of NBA-1S and NBA-2S ceramics at 200 °C

the observed density values of 95% TD for NBA-2S and 87% TD for NBA-1S ceramics. XRD patterns of NBA-2S and NBA-1S samples after densification are shown in Fig. 7. The intense XRD peak at 7.8° can be observed and it was formed is probably due to a strong orientation and growth of crystallites [18]. NBA-2S ceramics are found to be phase pure and also more crystalline in comparison to NBA-1S sample which may be due to the previous exposure to high temperature. SEM image on the polished surface of the sintered NBA-2S tube is shown in Fig. 8. The sample has shown exaggerated grain growth, though small size grains are also seen with well packed facets complementing the observed density of 95% TD.

Figure 9 shows the Cole-Cole plots of NBA-1S and NBA-2S samples measured at 200 °C. The plots contain two semicircles indicating the contribution of grain and grain boundaries to the conduction. The complex impedance plot at lower temperatures, shown in Fig. 10a, for NBA-2S sample exhibited deviated semicircle. On the other hand, complex impedance plots measured at high temperatures have shown two semicircles. In addition, the major contribution for conduction is found to be due to grains. Hence, the material impedance of the sample could be properly resolved into two semicircles and is fitted to equivalent circuit of two parallel RC combinations as shown in Fig. 10b. This indicates the contribution of grain and grain boundary conduction to the total conduction in this material system [19,20]. Ionic conductivities are calculated by measuring the low frequency intercepts for both the plots. AC conductivity is found higher in NBA-2S compared to NBA-1S ceramics. This may be due to enhanced NBA phase purity and crystallinity in combination with relatively higher density and dense microstructure. The so obtained conductivity for NBA-2S ceramics were 3×10^{-5} S/cm (at RT) and 6×10^{-5} S/cm (at 300 °C). Barison *et al.* [18] reported the conductivity of 2.6×10^{-6} S/cm (at 300 °C) in Mg doped BASE. In another work, Lu *et al.* [23] reported the conductivity of 12×10^{-4} S/cm (at RT) and

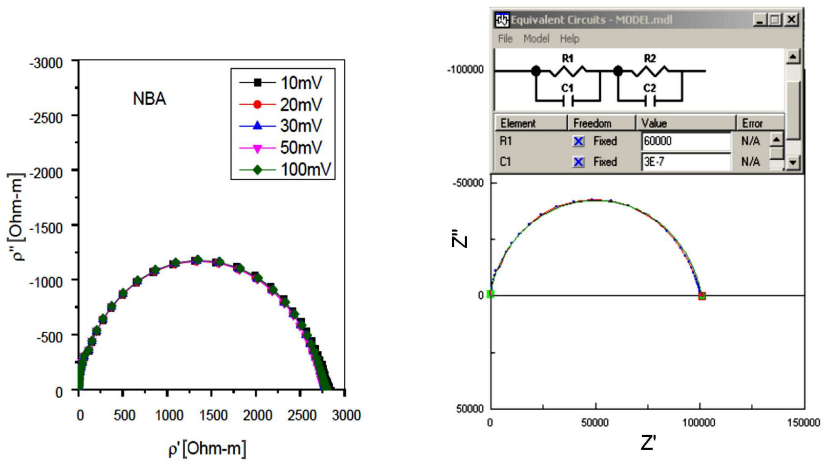

(a) (b)

Figure 10. Cole-Cole measured and fitted plots at different AC amplitudes (a) and equivalent circuit for NBA-2S ceramics (b)

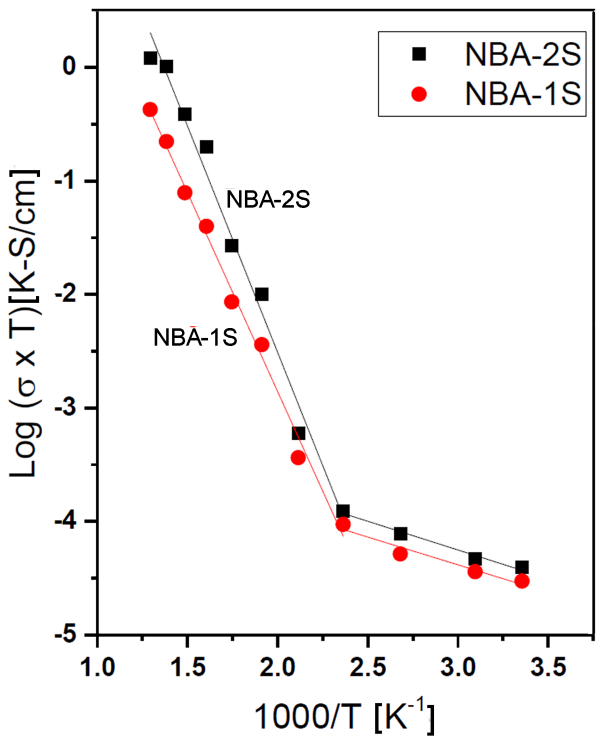

Figure 11. Arrhenius plots of NBA-1S and NBA-2S ceramics

65×10^{-3} S/cm (at 300 °C). In the present study, the differences in conductivity values were consistent with the earlier reports and also with the density values, phase and microstructure [4,18,21,22]. Moreover, the variation in conductivity with frequency of NBA-1S and NBA-2S ceramics were also studied. AC conductivity increased marginally with frequency in the low frequency region and increased significantly in the high frequency region. Figure 11 shows the variation of AC conductivity (σ_{AC}) with temperature of NBA-2S and NBA-1S ceramics. The AC conductivity pattern indicates a marginal rise in conductivity with temperature in the low temperature region and with considerable rise in conductivity at higher temperatures. The activation energy (E_a) has been calculated from the slope of a straight line in the low and high temperature regimes. The activation energies calculated from the AC conductivity plots are in the range of 0.64–0.74 eV in the high temperatures and are consistent with the reported values [18]. From the results of AC conductivity and the value of the activation energy for conduction, Na^+ ion conduction in NBA samples is clearly suggested.

IV. Conclusions

Pure and Li-doped sodium β-alumina ($NaMg_{0.67}Al_{10.33}O_{17}$) ceramics were prepared from the stoichiometric mixture of raw powders. Pellets and tubes are formed from the precursors (NBA-1S) and preformed sodium β-alumina powder (NBA-2S) through compaction and extrusion processing respectively. The specimens were finally sintered to dense ceramics. NBA-2S tubes and pellets exhibited high density values of 94–95% TD in comparison to NBA-1S samples which have shown a density of 85–87% TD of the theoretical density. Fractographs as well as microstructure complemented the observed density values. Cole-Cole plots exhibited two semicircles indicating the contribution of grain and grain boundary conductions. NBA-2S sample has shown higher AC conductivity at all the temperatures with the activation energy in the range of 0.64–0.74 eV, suggesting Na^+ ion conduction. The higher conductivity observed with NBA-2S sample compared to NBA-1S can be attributed to the relatively high phase purity and higher density, which enhances the Na^+ ion conduction.

Acknowledgements: The authors are grateful to SAIF, Kochi for providing the instrumental data, UGC and to the Principal, CMS College, Kottayam, Kerala for providing the necessary facilities.

References

1. K. Terabe, S. Yamaguchi, Y. Iguchi, I. Imai, "Characterization of sodium b-alumina prepared by sol-gel method", *Solid State Ionics*, **40-41** (1990) 111–114.
2. R.A. Pett, A.N. Theodore, "Preparation of beta alumina tubes by the extrusion process", Ford Motor Company of Canada Limited, Patent CA 1185771 A1, 1985.
3. M. Mikkor, "Sodium sulfur battery seals", Ford Motor company US Patent, 4 245 012 A, 1981.
4. X. Lu, G. Xia, J.P. Lemmon, Z. Yang, "Advanced materials for sodium-beta alumina batteries: Status, challenges and perspectives", *J. Power Sources*, **195** (2010) 2431–2442.
5. R. Subasri, "Investigations on the factors assisting a one-step synthesis cum sintering of sodium beta alumina using microwaves", *Mater. Sci. Eng. B*, **112** (2004) 73–78.
6. R. Subasri, T. Mathews, O.M. Sreedharan, V.S. Raghunathan, "Microwave processing of sodium beta alumina", *Solid State Ionics*, **158** (2003) 199–204.
7. A.K. James, P. Shiyou, "The crystal structure of Hydrated sodium aluminate $NaAlO_2 \cdot \frac{5}{4} H_2O$ and its dehydration product", *J. Solid State Chem.*, **115** [1] (1995) 126–139.
8. M. Bettman, C.R. Peters, "Crystal structure of $Na_2O \cdot MgO \cdot 5\,Al_2O_3$ (sodium oxide-magnesia-alumina) with reference to $Na_2O \cdot 5\,Al_2O_3$ and other isotypal compounds", *J. Phys. Chem.*, **73** (1969) 1774–1780.
9. H. Friedrich, "Spinel block doping and conductivity of sodium beta alumina ceramics", *Solid State Ionics*, **13** (1984) 53–61.
10. A. Mali, A. Petric, "Synthesis of sodium β''-alumina powder by sol-gel combustion", *J. Eur. Ceram. Soc.*, **32** (2012) 1229–1234.
11. J.L. Sudworth, A.R. Tilley, *The sodium sulphur battery*, Chapman and Hall, University Press, Cambridge, 1985.
12. J.L. Sudworth, "The sodium sulphur battery", *J.*

Power Sources, **11** [1-2] (2001) 143–154.
13. R.S. Gordon, R.W. Sutton, G.J. Tennenhouse, "Method for preparing shaped, green ceramic compacts", US Patent 4 020 134, 1977.
14. R. Gordon, B. Mc Entire, M. Miller, A. Virkar, "Processing and characterization of polycrystalline β''-alumina ceramic electrolytes", *Mater. Sci. Res.*, **11** (1978) 405–420.
15. M. Swathi, R. Papitha, U.S. Hareesh, B.P. Saha, R. Johnson, M. Vijaya Kumar, "Rheological studies on aqueous alumina extrusion mixes", *Trans. Ind. Inst. Met.*, **64** (2011) 541–547.
16. T. Oshima, M. Kajita, A. Okuva, "Development of sodium sulfur batteries", *Int. J. Appl. Ceram. Tech.*, **1** (2004) 269–276.
17. Y. Sakka, A. Honda, T.S. Suzuki, Y. Moriyoshi, "Fabrication of oriented β-alumina from porous bodies by slip casting in a high magnetic field", *Solid State Ionics*, **172** (2004) 341–347.
18. S. Barison, S. Fasolin, C. Mortalo, S. Boldrini, M. Fabrizio, "Effect of precursors on b-alumina electrolyte preparation", *J. Eur. Ceram. Soc.*, **35** [7] (2015) 2099–2107.
19. M. Haritha, M.B. Suresh, R. Johnson, "Synthesis and evaluation of thermal, electrical and electrochemical properties of $Ba_{0.5}Sr_{0.5}Co_{0.04}Zn_{0.04}Fe_{0.8}O_{3-\delta}$ as a novel cathode material for IT-SOFC application", *Ionics*, **18** [9] (2012) 891–898.
20. M.B. Suresh, R. Johnson, "The effect of strontium doping on densification and electrical properties of $Ce_{0.8}Gd_{0.2}O_{2-\delta}$ electrolyte for IT-SOFC application", *Ionics*, **18** [3] (2012) 281–297.
21. S.J. Allen, A.S. Cooper, F. De Rosa, J.P. Remeika, S.K. Olasi, "Far-infrared absorption and ionic conductivity of Na, Ag, Rb and K β-alumina", *Phys. Rev. B*, **17** (1978) 4031–4042.
22. A. Hooper, "A study of the electrical properties of single-crystal and polycrystalline β-alumina using complex plane analysis", *J. Phys. D: Appl. Phys.*, **10** (1977) 1487–1496.